Characterisation of a grooved heat pipe with an anodised surface

A. Brusly Solomon[a,b,*], A.M. Ram Kumar[c], K. Ramachandran[d], B.C. Pillai[a], C. Senthil Kumar[e], Mohsen Sharifpur[b], Josua P. Meyer[b]

[a] *Centre for Research in Material Science and Thermal Management, Department of Mechanical Engineering, Karunya University, Coimbatore, India*

[b] *Department of Mechanical and Aeronautical Engineering, University of Pretoria, Pretoria, South Africa*

[c] *Department of Mechanical Engineering, KSR Institute for Engineering and Technology, Namakkal, India*

[d] *Department of Physics, Bharathiar University, Coimbatore, India*

[e] *Department of Mechanical Engineering, SNS College of Technology, Coimbatore, India*

Abstract

A grooved heat pipe (GHP) is an important device for managing heat in space applications such as satellites and space stations, as it works efficiently in the absence of gravity. Apart from the above application, axial GHPs are used in many applications, such as electronic cooling units for temperature control and permafrost cooling. Improving the performance of GHPs is essential for better cooling and thermal management. In the present study, the effect of anodization on the heat transfer characteristics of a GHP is studied with R600a as a working fluid. In addition, the effects of fill ratio, inclination angle and heat inputs on the heat transfer performance of a GHP are studied. Furthermore, the effect of heat flux on dimensional numbers, such as the Webber (We), Bond (Bo), Kutateladze (Ku) and condensation (Co) numbers, are studied. The inclination angle, heat input and fill ratio of GHPs are varied in the range of 0 to 90^{o}, 25 to 250 W and 10 to 70% respectively. It is found that the above parameters have a significant effect on the performance of a GHP. Due to the anodisation, the maximum enhancement in heat transfer coefficient at the evaporator is 39% for a 90^{o} inclination at a heat flux of 11 kW/m^2. The reported performance enhancement of a GHP may be due to the large numbers of nucleation sites created by the anodisation process and enhancement in the capillary force due to the coating.

Keywords: Anodised GHP, grooved wick, nucleation site, capillary force, heat transfer coefficient, thermal resistance

1. Introduction

The heat pipe is a passive heat transfer device with high heat transport capabilities that can transfer heat over a long distance with a small temperature drop. The principle, operation and heat transfer limitations of heat pipes are well known. Heat pipes have emerged in various designs and are named thermosyphons (wickless heat pipes), capillary pumped loops (CPLs), loop heat pipes (LHPs), pulsating heat pipes (PHPs), grooved heat pipes (GHPs) and micro heat pipes (MHPs). The above mentioned heat pipes are specifically designed for certain applications. Among them, axial GHPs are receiving much attention in the field of aerospace, satellites and international space stations due to their high heat transport capability in the absence of gravity. Since a light weight is desirable, aluminium heat pipes are mostly used in these applications. As the technology of electronics systems advances faster in space applications, the use of an efficient heat transfer device is essential. Hence, a heat transfer device, such as a GHP, has to be improved with qualities such as a high heat transfer coefficient, shorter response time and compact structure.

Many techniques are used to improve the performance of GHPs by varying working fluids, wick structure and enhancing the inner surface area of an enclosure. A significant amount of heat transfer enhancement was found in GHPs when nanofluids were used as the working fluid. Shukla et al. [1] presented the heat transfer characteristics of screen meshed heat pipes with copper/water nanofluid as the working fluid. They reported that the efficiency of the heat pipe is enhanced by 14% compared to the heat pipe charged with DI water. Wang et al. [2] studied the operational characteristics of cylindrical GHPs using a CuO nanofluid as the working fluid. They found that the total resistance of a heat pipe charged with nanofluid is reduced by 50% compared to that of a heat pipe charged with water. The maximum heat transfer capacity of a heat pipe

charged with nanofluid was also enhanced by up to 40% compared with a heat pipe charged with water. Liu et al. [3] studied the effect of inclination angle on the performance of a GHP with a CuO nanofluid as the working fluid. They found that the performance of the inclined GHP can be strengthened with the use of a CuO nanofluid. Kumar et al. [4] studied the performance of heat pipes with a mixture of copper nanofluid and long chain alcohols. Results showed that the overall heat transfer coefficient and thermal efficiency of the heat pipe is enhanced with the use of nanofluids with long chain alcohols when compared to a heat pipe with nanofluids alone. Nazarimanesh et al. [5] studied the heat transfer performance of a U-shaped heat pipe with silver nanofluid as the working fluid. They found that the thermal resistance of a heat pipe with 50 ppm silver nanofluid is reduced by 40% compared with a heat pipe with water. Further, Liu et al. [6] noticed that the surface structure formed by a nanoparticle layer is responsible for the performance variation while using CuO nanofluid as the working fluid.

The type of wick structure, number of wick layers and flow behaviour in the heat pipes also plays a major role in the heat transfer enhancement [7]. From the inception of heat pipes, many types of wick structures were tested, including screen mesh, sintered wick, grooved wick, biporous wick and composite wick. Solomon et al. [8] studied the performance enhancement of a heat pipe with nanoparticle-deposited screen mesh as the wick material. Hopkins et al. [9] analysed the effect of rectangular and trapezoidal microgrooves on the heat transport capability of the heat pipe. Li et al. [10] performed a mathematical analysis to predict evaporation and condensation heat transfer in a copper/water heat pipe with sintered-grooved composite wick, and compared their predicted results with measured data. Wang et al. [11] analysed the heat transfer characteristics of flat heat pipes with interlaced narrow grooves or channels as the capillary structure. Wong and Chen [12] studied the performance of a grooved, flat-plate heat

pipe by visualisation with a powder-grooved evaporator in which metallic powder is filled in the grooves of the evaporator. Hu et al. [13] explored the effect of inner surface treatment on the performance of GHPs through a series of experiments. Lin et al. [14] tested an LHP with a bi-disperse wick structure and studied the effect of pore size on heat transfer. Wu et al. [15] developed and tested an LHP with a biporous wick structure and studied the heat transfer enhancement. Li et al. [16] tested an MHP by incorporating a compound structure of sintered wick on a grooved structure as the capillary material. From the studies [8–16], it is understood that the new kind of wick structures exhibited a significant effect on the heat transfer enhancement of heat pipes over the same with traditional wick structures. Although different wick structures are available for better heat transfer, the base materials of wick structures are mostly copper-based materials, which are slightly heavier than lightweight materials such as aluminium. Since heat pipes with a light weight are required for many applications, it is necessary to develop a lightweight aluminium-based wick structure. In this regard, Vasiliev et al. [17] developed an innovative heat pipe with a nanoparticle-deposited evaporator in which Al_2O_3 nanoparticles are deposited into the grooved surface. Although the heat transfer is enhanced considerably due to the coating, the proposed coating method is time-consuming and costly as the process involves two steps for the preparation and deposition of the nanoparticles. Hence, a cheaper technique to create such nanoporous deposits with a large number of micro/nanopores is utilised in aluminium thermosyphon and a better heat transfer was found compared with traditional thermosyphon [18, 19]. A similar technique is adopted to improve the performance of aluminium GHPs.

From the literature studied, it is understood that nanofluid plays an important role in enhancing the performance of heat pipes. However, due to the poor stability of nanofluids, the

long-term performance of heat pipes is not guaranteed. On the other hand, performance enhancement was found in heat pipes due to the deposition of the nanoparticles present in the nanofluids. Later, it was found that the artificial surface structure that formed inside the heat pipe wall also enhanced the performance of the heat pipe. These revelations lead to the development of advanced wick structures for heat pipes. It is also understood from the literature that the development of a wick from lightweight material is very important in many applications. Furthermore, the performance study of GHPs with an anodised inner surface is not reported in the open literature to the best of the authors' knowledge. Moreover, the anodisation process may reduce the width and contact angle (with working fluid) of the groove, which will enhance the capillary pressure. Therefore, the main objective of the present study is to fabricate a lightweight heat pipe with improved heat transfer performance and shorter response time by creating a thin porous coating using an anodising process. The effect of fill ratio and inclination angle on the thermal resistance of the GHP is also studied. Furthermore, the effect of anodisation on the evaporator and condenser heat transfer coefficients of anodised GHP is also reported.

2. Experimental details

In the present study, the GHP enclosure is prepared and all the heat transfer limitations of the GHP, such as viscous, entrainment, capillary, sonic and boiling limits, are considered. In order to make the heat transfer surface more effective, the anodisation process is performed after a necessary cleaning process. Next, scanning electron microscopy (SEM) images are taken to characterise the anodised surface. After ensuring a quality surface that is favourable for heat transfer enhancement, a GHP is fabricated and the experimental setup is done. Thereafter, the thermal instrumentation is carried out and experimental runs are conducted. The detailed steps involved in the fabrication of the anodised GHP and its testing are given in Section 2.1.

2.1 Fabrication and anodisation of GHP

An aluminium tube with an outside diameter of 19 mm, a length of 300 mm and a wall thickness of 1.4 mm is taken, and 24 axial grooves (rectangular in shape) are made on the inner wall using a wire-cutting process. The width and depth of the grooved structure are 0.8 mm. After making the grooved structure, the cleaning procedure for anodisation is followed. The cleaning process involves solid particle removal, chemical cleaning and desmutting. The detailed process of cleaning and anodising is found in the previous study [19, 20]. Later, anodisation is performed to coat the inner wall of the grooved surface. After this process has been completed, two ends of the grooved tube are sealed with end caps. One end cap carries the filling (capillary) tube for charging the working fluid. Finally, the GHP enclosure is subjected to a vacuum using a vacuum pumping system for up to one hour, and the working fluid is charged through a capillary tube by adjusting the valve arrangement. In this study, R600a is used as a working fluid, since it is compatible with an aluminium alloy.

The working fluid is charged while maintaining the temperature of the GHP between 2 and 5 ^{o}C, which makes the charging process easier by maintaining a low pressure in the GHP. The pressure in the GHP after charging is approximately 180450 Pas and the pressure in the GHP varies based on the temperature. The required amount of working fluid is ensured by weighing the GHP.

2.2 Experimental setup and testing

After the fabrication of the GHP, the experimental setup is made as shown in Figure 1. The experimental setup consists of a cooling system, chilling unit (0 to 25 ^{o}C), flow and cooling jacket, which are connected to the condenser of the heat pipe. The heating system consists of a variable transformer, digital voltmeter, digital ammeter and a heating

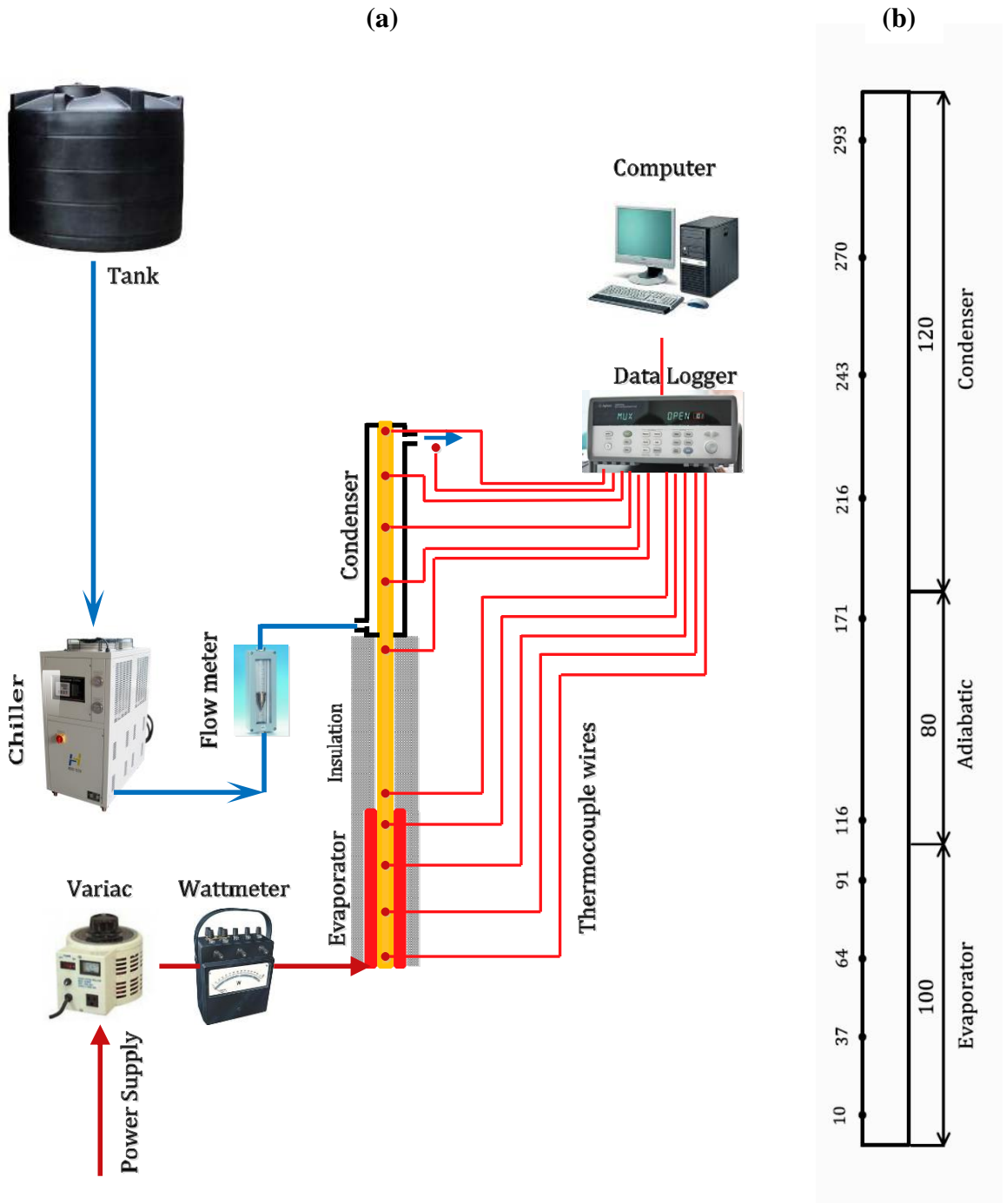

Figure. 1 Schematic view of (a) experimental setup; and (b) Thermocouple positions

element (1000 W). The data monitoring and recording system consists of thermocouples, a data logger (Agilent-34972A) and a personal computer. Heat input is given at the evaporator and cooling is provided in the condenser by supplying cooling water at a temperature of 15 ± 1 °C. The flow rate of the cooling water is maintained at 360 ml/min. An electrical resistance heating element is winded over the evaporator section and connected through a voltmeter and ammeter. Ten T-type thermocouples are welded over the surface of the GHP as shown in Figure 1b and the signals of the thermocouples are quickly recorded on the computer by the data acquisition system. The accuracy of the thermocouple is ± 0.2 °C, which includes the uncertainty of the data logger. The input power is increased up to 200 W with an increment of 25 W, and the wall temperature is recorded. The heat transferred by the GHP is estimated by Newton's law of cooling. The length of the evaporator, adiabatic and condenser sections of the heat pipe are taken as 100 mm, 80 mm and 120 mm, respectively. The uncertainty in the flow measurement is ±3%. The uncertainty in the measurement of temperature is ±0.5%.

3. Data reduction

In the present study, the heat input is calculated from the voltmeter and ammeter readings as:

$$Q_{in} = V.I \tag{1}$$

Heat transferred by the GHP is equal to the heat absorbed by the coolant fluid, which is calculated by the heat balance equation as:

$$Q_{out} = \dot{m}_{l}\, c_{p,l}\, (T_{out} - T_{in}), \tag{2}$$

where $\dot{m}_l$ and $c_{p,l}$ are the mass flow rate and heat capacity of the coolant, respectively. T_{out} and T_{in} are the temperature at the outlet and inlet of the cooling water, respectively. In order to access the performance of the GHP, the total thermal resistance of the GHP is estimated as:

$$R = \frac{\bar{T}_e - \bar{T}_c}{\dot{Q}_{out}}, \tag{3}$$

where $\bar{T}_e$ and $\bar{T}_c$ are the average evaporator and condenser wall temperatures of the GHP respectively. In addition, the heat transfer coefficients at the evaporator and condenser sections of the GHP are estimated using equations (4) and (5) respectively:

$$h_e = \frac{q_e}{T_{e,i} - T_{sat}} \quad , \tag{4}$$

where $q_e = \frac{Q_{in}}{2\pi r l_e}$, and Q_{in} is the heat input, which is calculated using Equation (1) ; and:

$$h_c = \frac{q_c}{T_{sat} - T_{c,i}} \tag{5}$$

where $q_c = \frac{Q_{out}}{2\pi r l_c}$.

The inner wall temperatures of the evaporator and condenser sections of the GHP are obtained using Fourier heat conduction equations (6) and (7) respectively:

$$T_{e,i} = \bar{T}_e + \frac{q r_o}{k} ln\left(\frac{r_i}{r_o}\right); \text{ and} \tag{6}$$

$$T_{c,i} = \bar{T}_c + \frac{q r_o}{k} ln\left(\frac{r_o}{r_i}\right). \tag{7}$$

The temperature at the adiabatic section of the GHP is assumed as a vapour temperature (T_{sat}) of the working fluid.

The uncertainties present in the measurement of heat flux and the heat transfer coefficient are calculated using equations (8) and (9) as [21]:

$$\frac{\Delta q}{q} = \sqrt{\left(\frac{\Delta Q}{Q}\right)^2 + \left(\frac{\Delta A}{A}\right)^2}; \text{ and} \tag{8}$$

$$\frac{\Delta h}{h} = \sqrt{\left(\frac{\Delta q}{q}\right)^2 + \left(\frac{\Delta(\Delta T)}{\Delta T}\right)^2}. \tag{9}$$

The uncertainty present in the measurements of the total resistance of both the anodised and non-anodised GHP is calculated as:

$$\frac{\Delta R}{R} = \sqrt{\left(\frac{\Delta Q}{Q}\right)^2 + \left(\frac{\Delta(\Delta T_{hp})}{\Delta T}\right)^2}. \tag{10}$$

The presence of uncertainties in the measurements of heat flux, heat transfer coefficient and total resistances are less than 6.5%.

4. Results and discussion

After the anodisation process, a piece of anodised tube is analysed using an SEM, and images of both anodised and non-anodised surfaces are compared. Figure 2 shows the SEM images of a non-anodised (a and c) and anodised (b and d) grooved surface. Due to the anodisation, a thin layer of Al_2O_3 microstructure, which may enhance the nucleation sites, is formed on the grooved surface (figures 2b and 2d). It is also noticed that the surface morphology of the grooved tube is altered with a rough surface that consists of a large number of pores and cracks. The pore size of the anodised grooved surface is estimated from Figure 2d and is in the range of 2 to 5 μm. These pores are likely to generate more number ofnucleation's and enhance the heat transfer. With this enhanced surface, the GHP's performance is studied. In the present

Non-anodised surface Anodised surface

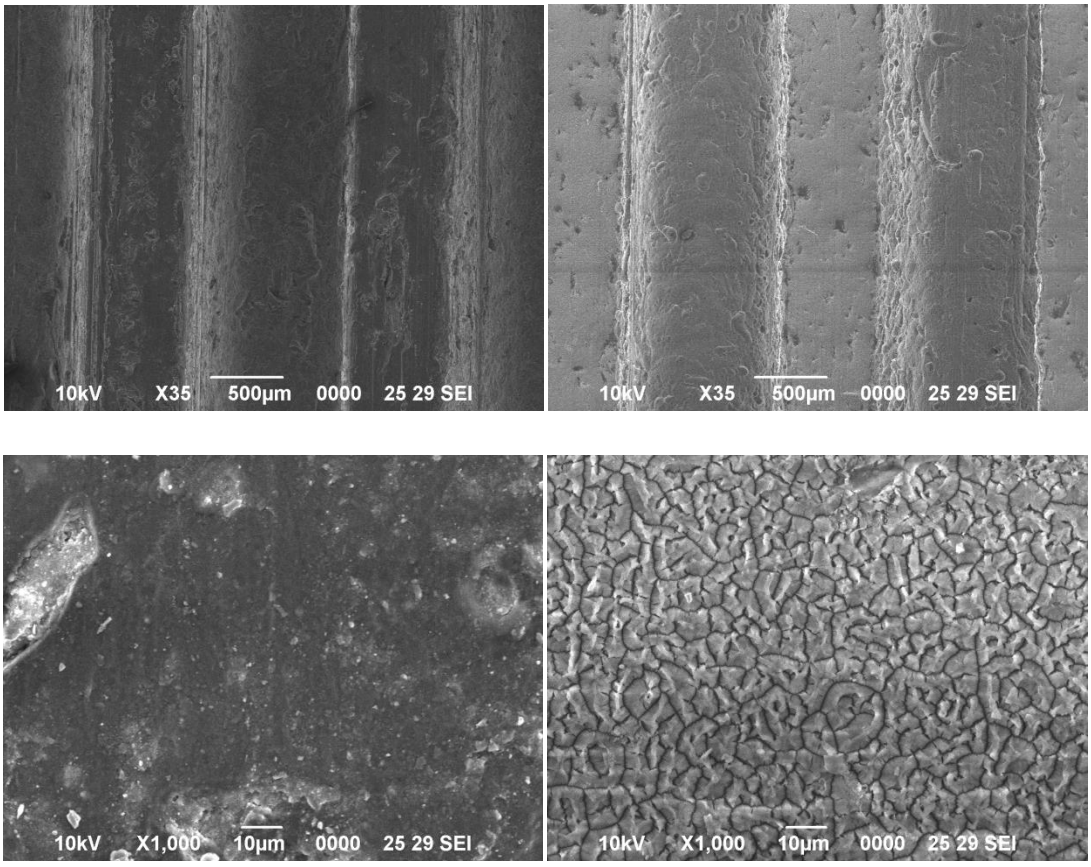

Figure. 2 SEM images of non-anodised and anodised surface of GHP

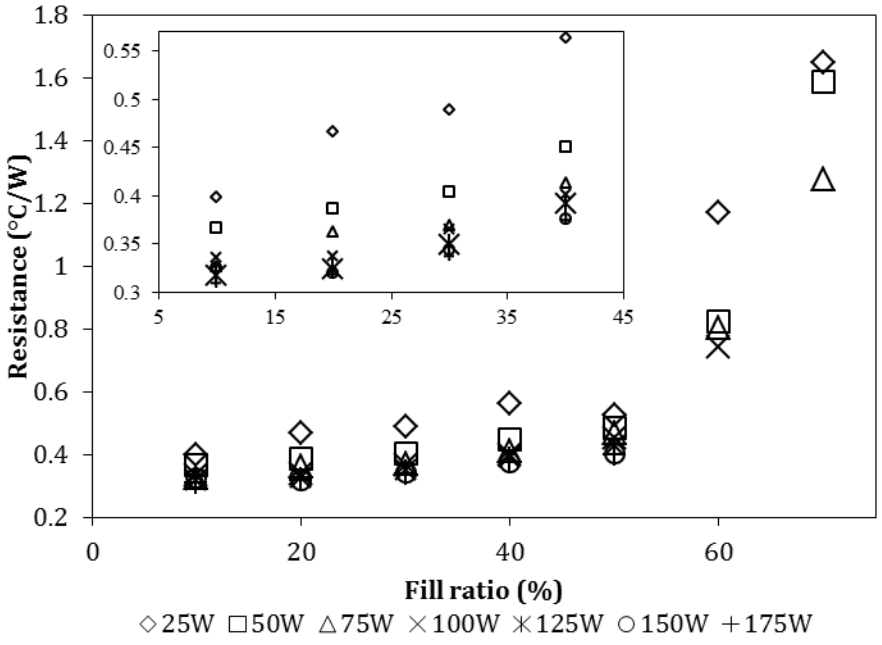

Figure. 3 Effect of fill ratio on the thermal resistance of non-anodised GHP

study, the fill ratio of working fluid is varied from 10 to 70%, which is estimated as the ratio of volume occupied by the working fluid to the total volume of the GHP. The inclination angle of the GHP is varied from 0 to 90^{o}. The total thermal resistance of the GHP is calculated using Equation (3) and is presented in Figure 3 for various fill ratios. The effect of the fill ratio on the thermal resistance is less significant at lower fill ratios and more significant at higher fill ratios. It is also found that the heat transfer capacity of the GHP at a lower fill ratio is higher and the same is lower at a higher fill ratio. Furthermore, thermal resistance is found to be uniform up to a fill ratio of 50%, and increases drastically above 50%. This shows that the GHP with refrigerant can operate effectively when the fill ratio is less than 50%. The higher fill ratio in heat pipes leads to a boiling limitation in which vapour formation occurs as a thin layer on the evaporator surface due to a high radial heat flux [18]. Since the thermal conductivity of the vapour is much smaller than in liquids, the heat transfer from the wall to the working fluid is limited, leading to an increase in the wall temperature. Finally, the 10% fill ratio of the working fluid is used in all the remaining experiments since low resistance is obtained in this fill ratio.

With the 10% fill ratio of the working fluid, the effect of the inclination angle on the thermal resistance of a GHP is studied and presented in Figure 4 (a and b). It is found that the inclination angle has a significant effect on the thermal resistance of a GHP. As the inclination angle increases, the thermal resistance decreases at all heat inputs. This may be due to the gravity effect on the liquid return. As the gravity effect increases, the liquid inventory in the evaporator also increases, which leads to better heat transport, resulting in lower resistance. Furthermore, it is seen that the thermal resistance of both non-anodised (Figure 4a) and anodised GHPs (Figure 4b) showed a similar profile. However, the resistance of the anodised GHP is lower than that of the non-anodised GHP. This resulted from the enhancement of boiling heat transfer in the

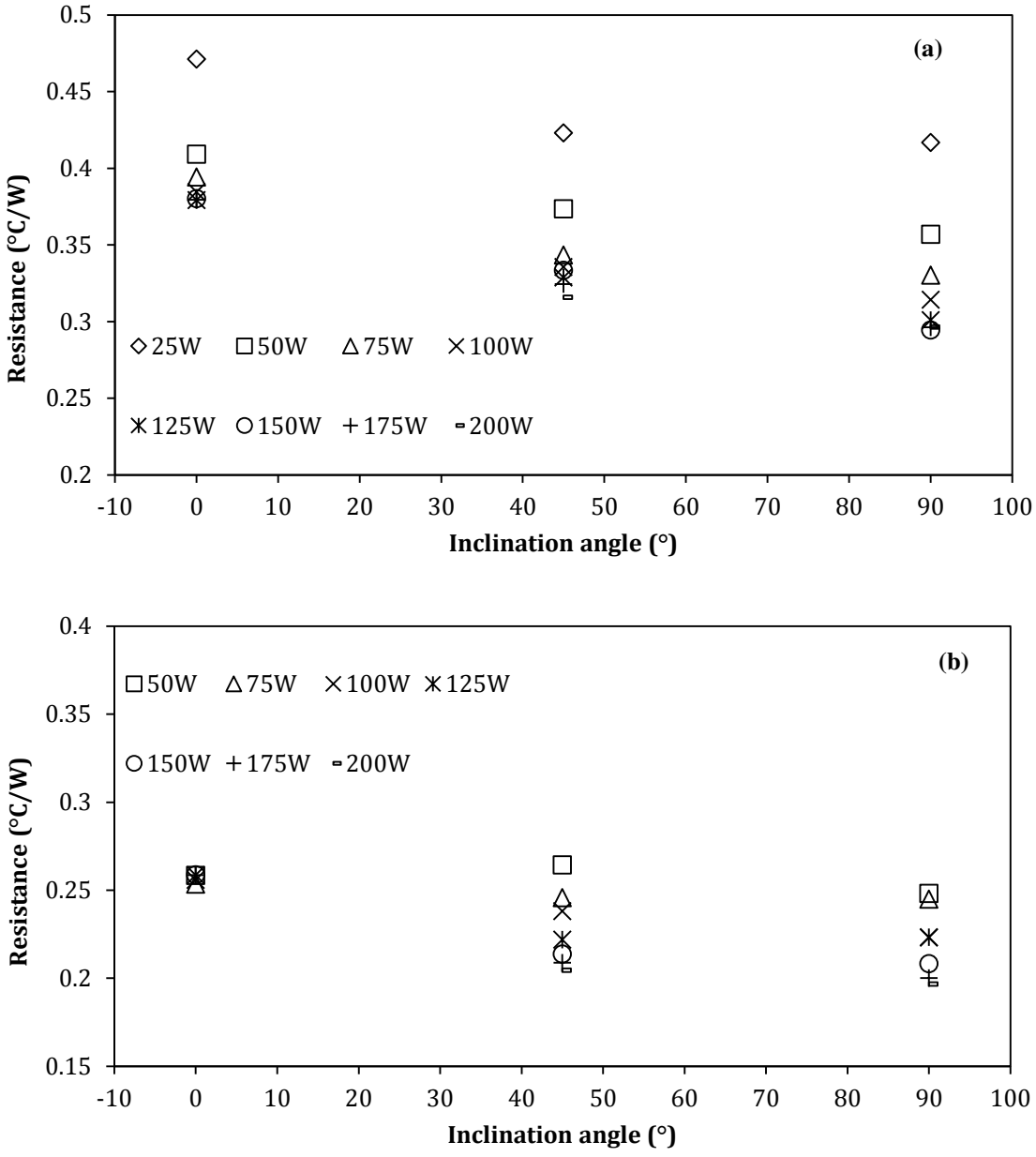

Figure. 4 Effect of inclination angle on the thermal resistance of (a) non-anodised; and (b) anodised GHP

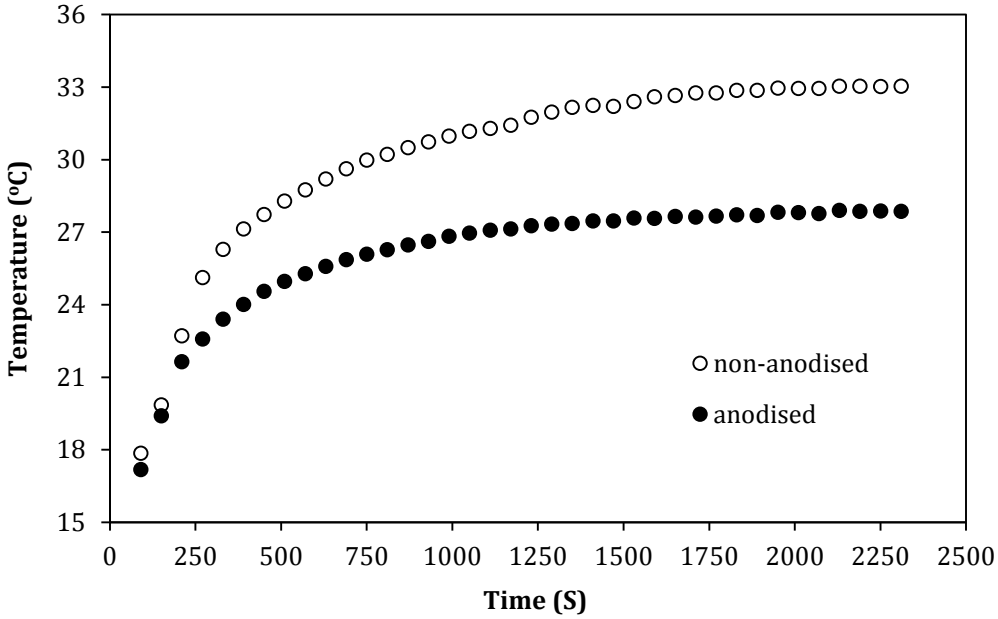

Figure. 5 Transient evaporator temperature response of GHPs

GHP evaporator. Moreover, the effect of input power on the thermal resistance increases as the input power for anodised and non-anodised GHPs decreases. However, the same is weaker in anodised GHPs.

In order to study the effect of anodisation on the heat transfer performance of GHPs, the average evaporator temperature during transient conditions and a steady state wall temperature along the length of the GHP are recorded and presented at an inclination angle of 90^{o}. Figure 5 shows the transient temperature profile at the evaporator of both anodised and non-anodised GHPs at 25 W. As time progresses, the evaporator's temperature increases for both the anodised and non-anodised cases, and reaches a maximum at a steady state. It is evident that the temperature response of the anodised GHP is shorter compared with the non-anodised GHP. Furthermore, non-anodised and anodised GHPs reached a steady state at 1 830 and 1 230 seconds respectively, which suggests that the anodised GHP is 30% quicker than the non-anodised GHP. Furthermore, the non-anodised GHP reached a steady state at 33 ^{o}C, whereas the anodised GHP reached a steady state at 28 ^{o}C. This resulted in a 15% reduction in the evaporator temperature and shows that the anodised GHP responds quickly and transfers heat more efficiently. This enhancement mainly occurs because of the enhanced heat transfer mechanisms due to anodisation.

Figures 6 a, b and c show the wall temperature of anodised and non-anodised GHPs at 50, 125 and 200 W respectively. As the heat input increases, the wall temperature also increases for both anodised and non-anodised GHPs. It was also found that the average wall temperature at the evaporator of an anodised GHP is lower than that of a non-anodised GHP at all heat inputs. However, the wall temperature at the condenser of an anodised GHP is higher than at a non-anodised GHP at lower heat inputs, and is almost the same at higher heat inputs. Furthermore, it

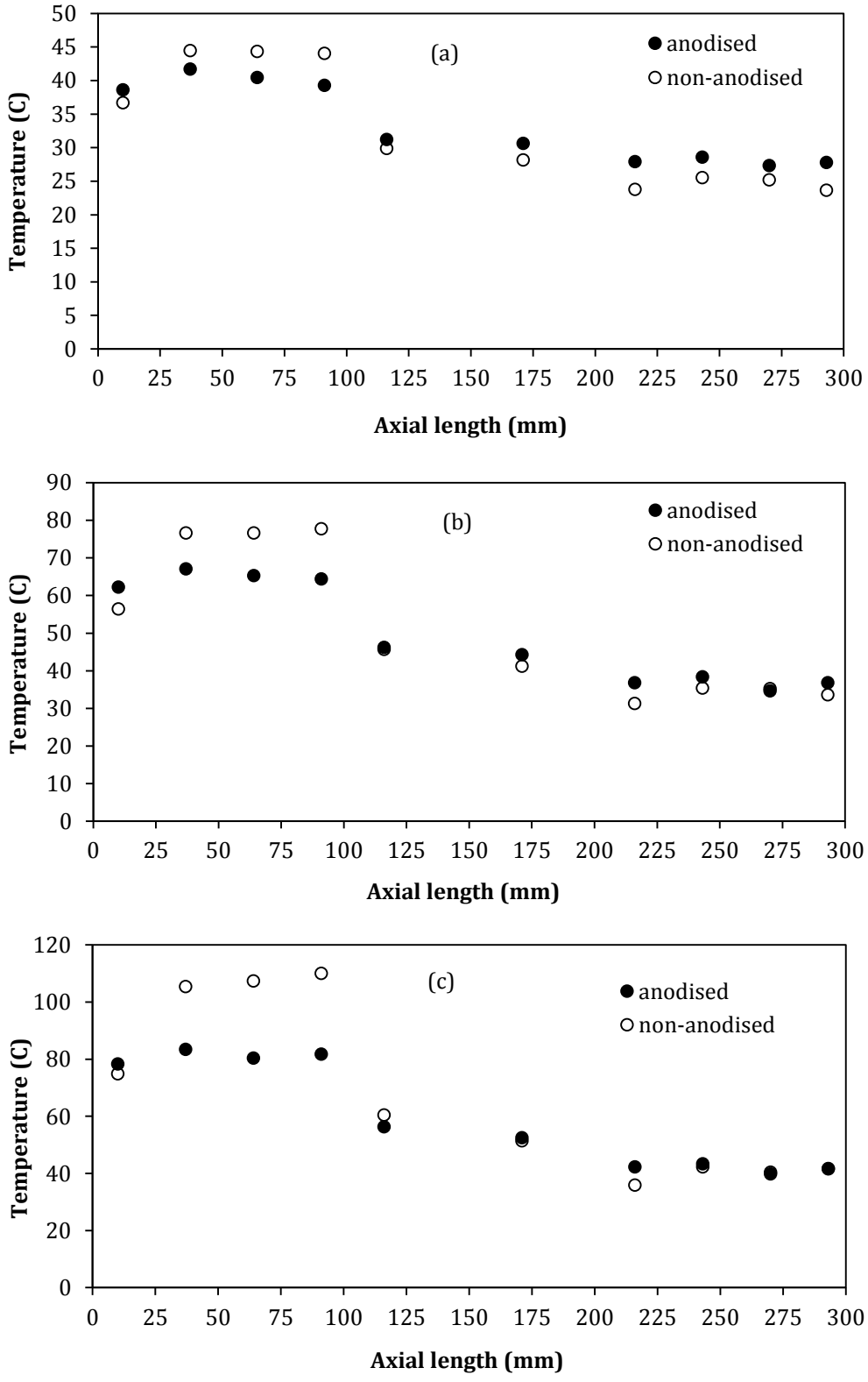

Figure. 6 Wall temperature profiles of anodised and non-anodised GHPs at (a) 50 W (b) 125 W and (c) 200 W

is noted that the temperature at the evaporator of a non-anodised GHP is not uniform, whereas the same is uniform in an anodised GHP. This is mainly due to the variation in the boiling mechanism of both anodised and non-anodised GHPs. The maximum reduction in the wall temperature at an anodised GHP evaporator is 18% when compared with a non-anodised GHP at a heat input of 200 W. Due to the anodisation process, an enormous number of small pores, as shown in Figure 1d, were created and act as nucleation sites that promote uniform nucleate boiling. Hence, the temperature at the evaporator of an anodised GHP is uniform. More details of nucleation effects on the heat transfer of an anodised surface were found in the previous studies [19, 20].

Figure 7 shows variations in the heat transfer coefficient at the evaporator of both an anodised and a non-anodised GHP at different heat fluxes. As expected, the heat transfer coefficient at the evaporator of the anodised GHP is higher than that of the non-anodised GHP. This is mainly due to the boiling enhancement in the evaporator of the anodised GHP, as explained earlier. It is also found that the effect of the inclination angle on the heat transfer coefficient is less significant for non-anodised GHPs, and the same is more significant for anodised GHPs. Furthermore, the heat transfer coefficient of the non-anodised GHP increases linearly up to 7 kW/m^2 and then decreases slightly. This shows that a non-anodised GHP does not effectively transfer the heat above 7 kW/m^2. It is interesting to note that the heat transfer coefficient of an anodised GHP still increases, even after a heat flux of 7 kW/m^2. This shows that the heat transfer capability of a GHP is enhanced by the anodising process. The maximum heat transfer coefficient enhancement in the evaporator of an anodised GHP is about 38% when compared to a non-anodised GHP working at a 90^o inclination at a heat flux of 11 kW/m^2.

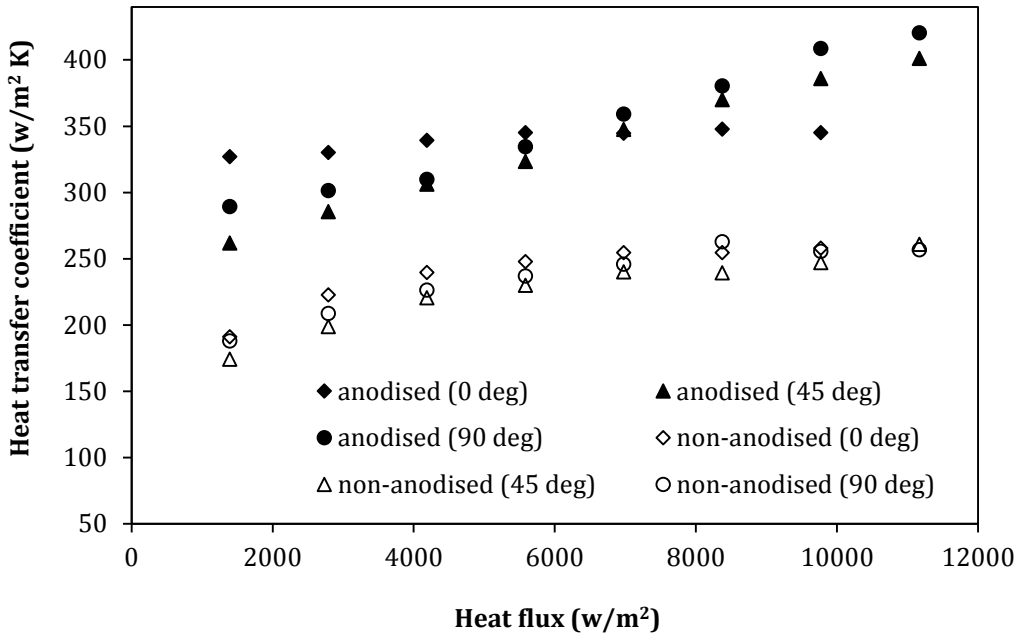

Figure. 7 Heat transfer coefficient at the evaporator of anodised and non-anodised GHP

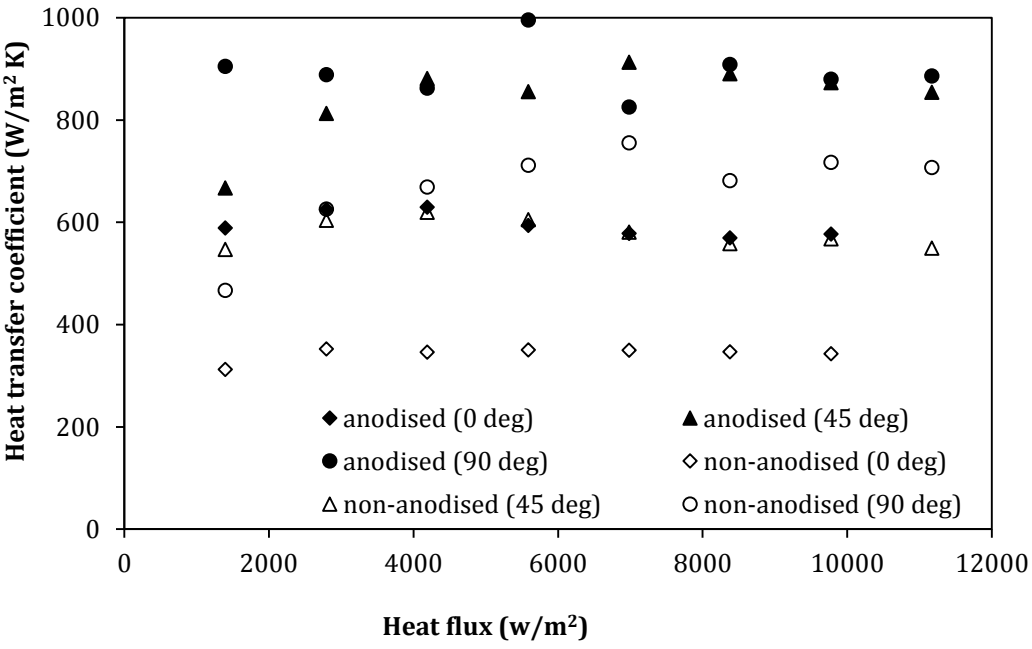

Figure. 8 Heat transfer coefficient at the condenser of anodised and non-anodised GHP

Moreover, the heat transfer coefficient of an anodised GHP at an inclination angle of 0^o is almost uniform. However, as the inclination angle increases, the heat transfer coefficient also varies with heat flux. At an inclination of 45 to 90^o, the heat transfer coefficient of the anodised GHP is lower than that obtained in the horizontal position (inclination of 0^o) at lower heat fluxes. In contrast, at the same inclination angle, the heat transfer coefficient is higher than that of the same at a horizontal position at higher heat fluxes. This is mainly because of the variation in the liquid inventory in the evaporator due to the effect of gravity. As the inclination angle increases, the liquid inventory in the evaporator also increases and offers additional resistance at lower heat fluxes due to the limited amount of fluid circulation. Hence, the heat transfer coefficient is lower compared with the heat transfer coefficient at a horizontal position. However, as the heat flux increases, the boiling rate also increases and the liquid pool vanishes due to the higher amount of fluid circulation, which results in lower resistance. Hence, the heat transfer coefficient increases at higher heat fluxes. Enhancing the capillary pressure is partly responsible for this variation in the heat transfer of an anodised GHP compared to a non-anodised GHP. When the anodisation is performed, the width of the grooved structure decreases slightly. This will increase the capillary pressure. Moreover, the contact angle plays a major role in enhancing the capillary pressure, since the capillary pressure is proportional to the contact angle. It is proven that the contact angle of an anodised surface is less than that of a non-anodised surface [16]. The capillary pressure generated in the grooved wick is represented as:

$$\Delta p = 2\,\sigma cos\theta / W \tag{11}$$

Based on Equation (11), the capillary pressure increases when the grooved width, as well as the contact angle, is decreased due to anodisation. This enhancement in the capillary pressure

leads to the enhancement of fluid circulation, which results in the enhancement of the heat transfer coefficient.

Figure 8 shows the heat transfer coefficient at the condenser of anodised and non-anodised GHPs at various heat fluxes. Similar to the evaporator, the heat transfer coefficient at the condenser of an anodised GHP is higher than that of a non-anodised GHP. Unlike the heat transfer coefficient variation at the evaporator section, the same in the condenser section is almost uniform as the heat input increases. When compared to the heat transfer coefficient at the evaporator and condenser of an anodised and a non-anodised GHP, the heat transfer coefficient in the condenser is higher than that of the evaporator. A similar pattern is seen in previous experimental studies of thermosyphons [20, 22]. This is mainly because of the heat transfer mechanism involved in a particular section of a heat pipe. Generally, heat transfer in the evaporator section takes place by nucleate or film boiling. On the other hand, heat transfer takes place by film condensation in the condenser section. It is known that the heat transfer coefficient of the film condensation process is higher than that of the nucleate boiling process [23]. Therefore, the heat transfer coefficient in the condenser section is higher than in the evaporator. Further, the maximum heat transfer coefficient enhancement in the condenser of an anodised GHP is about 20% when compared with a non-anodised GHP working at 90^{o} inclination at a heat flux of 11 kW/m^2.

The total thermal resistance of both anodised and non-anodised GHPs at various heat inputs is presented in Figure 9. It can be seen that the thermal resistance of an anodised GHP is lower than that of a non-anodised GHP. At all inclination angles of the non-anodised GHP, the total resistance exponentially decreases with heat input up to 125 W and then it is constant, even as the heat input is increases. However, the total resistance of an anodised GHP at a horizontal

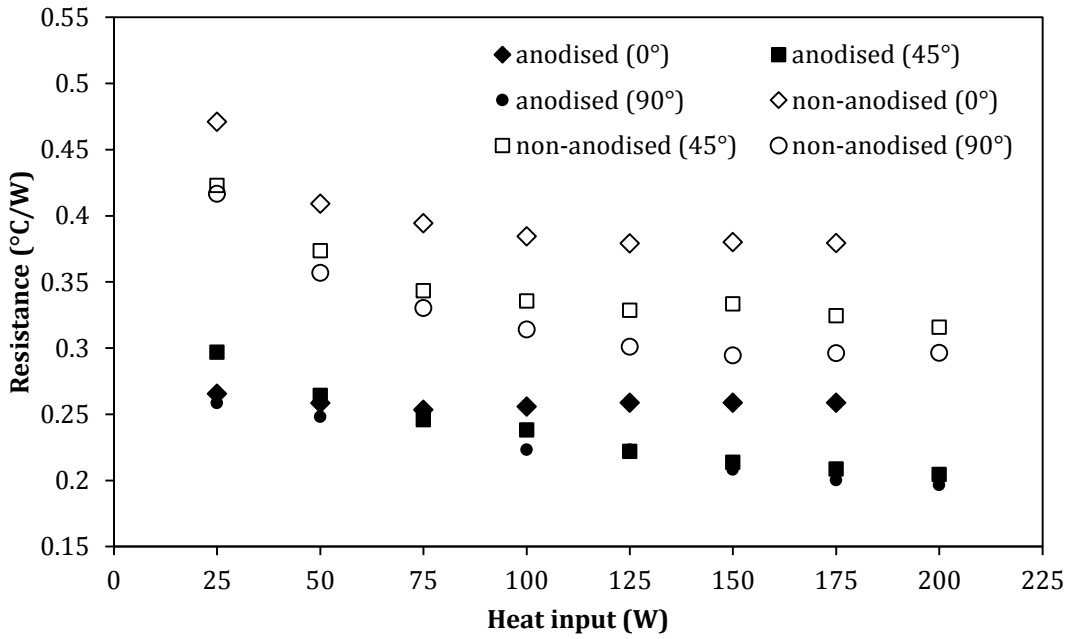

Figure. 9 Variations in the total thermal resistance of anodised and non-anodised GHP

position is almost uniform, and for other inclination angles, the total resistance of the GHP is linearly decreased with heat input. It was also found that the total resistance of an anodised GHP reduces by 33% compared to a non-anodised GHP at 200 W for the inclination angle of 90^{o}. This shows that the anodisation process significantly decreases the thermal resistance of GHPs and enhances the heat transfer performance of the same.

Furthermore, to analyse the influence of anodisation on the heat transfer enhancement process in the GHP, non-dimensional numbers such as Webber (We), Bond (Bo), Kutateladze (Ku) and condensation (Co) numbers are used. The thermo-physical properties of R600a are taken from the ASHRAE hand book [24] at the average adiabatic temperature of GHP which is assumed as the vapour temperature. Figure 10a shows the effect of heat flux on the Bo. The Bo is the ratio of buoyancy force to the surface tension force. When the temperature increases, the surface tension decreases, which leads to more buoyancy and vigorous boiling. Therefore, the Bo represents the boiling phenomenon in the GHP. Generally, if the Bo is high, the boiling is more intense. Figure 10a shows that the Bo increases as the heat flux increases, which indicate that the boiling is even more intense as the heat flux increases. It can also be seen that the Bo for an anodised surface is higher than that of a non-anodised surface, which indicates that the boiling is more vigorous in the anodised surface than in the non-anodised surface.

Figure 10b shows the effect of heat flux on the We of the GHP. The We represents the counter-current interactions between the free surface of liquid film and vapour flows inside the evaporator and condenser of the GHP. Figure 10b shows that the counter-current interactions increase as the heat flux increases, which bodes well for the improved operation of the GHP. It is also noticed that the anodised GHP shows a higher We, which indicates that the counter-current interactions are better than for a non-anodised GHP, and offers more free surfaces, leading to

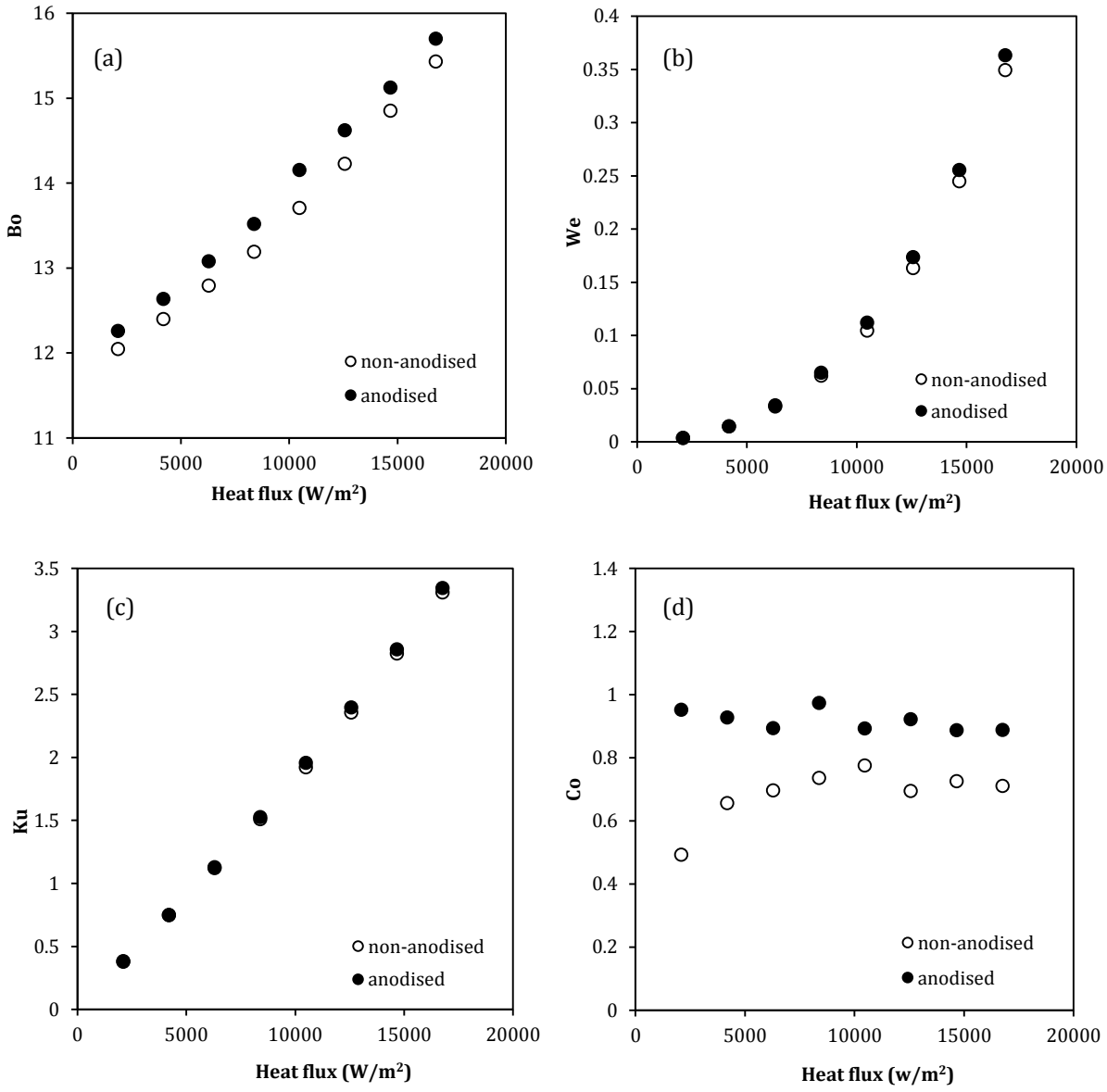

Figure. 10 Effect of heat flux on the non-dimensional numbers (a) Bond (b) Webber (c) Kutateladze; and (d) Condensation number

higher heat transfer. The enhancement in counter-current interaction reduces the chances of flooding as the working fluid is circulated efficiently to the evaporator.

The effect of heat flux on the Ku is presented in Figure 10c. The Ku represents the pool-boiling occurrence in the liquid pool of the GHP evaporator. From Figure 10c, it is seen that the Ku increases linearly with the heat flux for both anodised and non-anodised GHPs. This suggests that the pool-boiling enhances with heat flux. It is also found that the Ku of an anodised GHP is slightly higher than the Ku of a non-anodised GHP. This represents the better pool-boiling characteristics of the anodised GHP.

The effect of heat flux on the Co is presented in Figure 10d and the Co represents the amount of liquid that returns to the GHP evaporator. Figure 10d shows that the Co of the non-anodised GHP is lower at low heat fluxes and increases as the heat flux increases to a certain level. It remained constant at higher heat fluxes. In the case of an anodised GHP, the Co is high in the lower heat flux and remains almost constant as the heat flux increases. This reveals that the condensate return increases considerably with the use of an anodised surface. From this study, the decrease in the evaporator wall temperature as well as the total resistance, increase in the heat transfer coefficient of both the evaporator and the condenser, enhancement in the non-dimensional numbers clearly indicates that the performance of the GHP is enhanced due to the anodisation process.

5. Conclusion

The effect of anodisation on the heat transfer performance of GHPs is studied. The effect of fill ratio, inclination angle and heat input on the performance of a GHP is also studied. An anodised surface provides an additional capillary pressure to circulate the working fluid

efficiently from the condenser to the evaporator. Furthermore, a large number of nucleation sites produced during the anodisation process promotes nucleate boiling and enhances heat transfer between the wall and the working fluid. Due to this action, the heat transfer coefficient of the GHP at both the evaporator and condenser are drastically increased. Compared to the thermal resistance of a non-anodised GHP, a reduction of almost 37% is observed for an anodised GHP at an inclination of 90^{o} with a heat input of 25 W. As the anodised GHP possesses high heat transfer characteristics with shorter response time and is lightweight in nature, it is suitable for space applications, including electronics cooling in space and cabin temperature control. Also, reduction in weight of GHP leads to reduction in payload that saves launching cost considerably.

Acknowledgement

The authors appreciate the technical assistance of Mr Jeyaseelan of the Centre for Research in Material Science and Thermal Management, Karunya University, during fabrication and testing.

References

[1]. Shukla KN, Solomon AB, Pillai BC, Ibrahim M (2010) Thermal performance of cylindrical heat pipe using nanofluids. Journal of Thermophysics and Heat Transfer 24:796–802.

[2]. Wang G-S, Song B, Liu Z-H (2010) Operation characteristics of cylindrical miniature grooved heat pipe using aqueous CuO nanofluids. Experimental Thermal Fluid Science 34:1415–1421.

[3]. Liu Z-H, Li Y-Y, Bao R (2010) Thermal performance of inclined grooved heat pipes using nanofluids. International Journal of Thermal Science 49:1680–1687.

[4]. Kumar RS, Vaidyanathan S, Sivaraman B (2015) Effect of copper nanofluid in aqueous solution of long chain alcohols in the performance of heat pipes. Heat Mass Transfer 51: 181–193.

[5]. Nazarimanesh M, Yousefi T, Ashjaee M (2015) Experimental investigation on the effect of nanofluid on the thermal performance of symmetric sintered U shaped heat pipe. DOI 10.1007/s00231-015-1644-x.

[6]. Liu Z-H, Li Y-Y, Bao R (2011) Compositive effect of nanoparticle parameter on thermal performance of cylindrical micro-grooved heat pipe using nanofluids, International Journal of Thermal Science 50:558–568.

[7]. Abo El-Nasr A, El-Haggar SM (1996) Effective thermal conductivity of heat pipes. Heat Mass Transfer 32:97–101.

[8]. Solomon AB, Ramachandran K, Pillai BC (2012) Thermal performance of a heat pipe with nanoparticles coated wick. Applied Thermal Engineering 36:106–112.

[9]. Hopkins R, Faghri A, Khrustalev D (1999) Flat miniature heat pipes with micro capillary grooves. Journal of Heat Transfer 121:102–109.

[10]. Li Y, He H-F, Zeng Z-X (2013) Evaporation and condensation heat transfer in a heat pipe with a sintered-grooved composite wick. Applied Thermal Engineering 50:342–351.

[11]. Wang C, Liu Z, Zhang G, Zhang M (2013) Experimental investigations of flat plate heat pipes with interlaced narrow grooves or channels as capillary structure. Experimental Thermal Fluid Science 48:222–229.

[12]. Wong S-C, Chen C-W (2013) Visualisation experiments for groove-wicked flat-plate heat pipes with various working fluids and powder-groove evaporator. International Journal of Heat Mass Transfer 66:396–403.

[13]. Hu Y, Cheng J, Zhang W, Shirakashi R, Wang S (2013) Thermal performance enhancement of grooved heat pipes with inner surface treatment. International Journal of Heat Mass Transfer 67:416–419.

[14]. Lin F-C, Liu B-H, Juan C-C, Chen Y-M (2011) Effect of pore size distribution in bidisperse wick on heat transfer in a loop heat pipe. Heat Mass Transfer 47:933–940.

[15]. Wu SC, Hsieh BH, Wang D, Chen YM (2015) Manufacture of a biporous nickel wick and its effect on LHP heat transfer performance enhancement. Heat Mass Transfer 51: 1549–1558.

[16]. Li X, Li M, Li M, Wu R, Wan Y, Cheng T (2015) Forming method of micro heat pipe with compound structure of sintered wick on grooved substrate. Heat Mass Transfer. DOI 10.1007/s00231-015-1585-4.

[17]. Vasiliev L, Grakovich L, Rabetsky M, Romanenkov V, Vasiliev L, Ayel V, Bertin Y, Romestant C, Hugon J (2010) Grooved heat pipes with nanoporous deposit in an evaporator. Heat Pipe Science and Technology 1:219–236.

[18]. Faghri A (1995) Heat pipe science and technology. London: Taylor and Francis.

[19]. Solomon AB, Mathew A, Ramachandran K, Pillai BC, Karthikeyan VK (2013) Thermal performance of anodised two phase closed thermosyphon (TPCT). Experimental Thermal Fluid Science 48:49–57.

[20]. Solomon AB, Roshan R, Vincent W, Karthikeyan VK, Asirvatham LG (2015) Heat transfer performance of an anodized two-phase closed thermosyphon with refrigerant as working fluid. Internationa Journal of Heat Mass Transfer 82:521–529.

[21]. Holmon JP, Experimental Methods for Engineers, 8th Edition. New York, NY: McGraw-Hill.

[22]. Huminic G, Huminic A (2011) Heat transfer characteristics of a two-phase closed thermosyphons using nanofluids. Experimental Thermal Fluid Science 35:550–557.

[23]. Lienhard IV JH, Lienhard V JH (2003) A heat transfer text book, 3rd Edition, pp. 21. Cambridge, MA: Phlogiston Press.

[24]. ASHRAE Hand Book (2009) Chapter 30-Thermophysical Properties of Refrigerants, pp. 30.49

Nomenclatures

Bo	Bond number $\left(D\left[g\frac{\rho_l-\rho_v}{\sigma}\right]^{\frac{1}{2}}\right)$
$c_{p,l}$	specific heat of coolant fluid (J/kg K)
Co	Condensation number $\left(\frac{h}{k}\left[\frac{\mu^2}{g\rho^2}\right]^{\frac{1}{3}}\right)$
D	diameter (m)
h	heat transfer coefficient (W/m^2 K)
I	current (A)
T	temperature (^{o}C)
k	thermal conductivity (W/m K)
l	length (m)
$\dot{m}_l$	mass flow rate of coolant (kg/s)
Ku	Kutateladze number $\left[\frac{q}{\left[\rho_v h_{fg}\left(\frac{\rho_l-\rho_v}{\rho_v^2}\right)\right]^{\frac{1}{4}}}\right]$
Q	heat transfer rate (W)
q	heat flux (W/m^2)
R	resistance (^{o}C/W)
r	radius(m)
V	voltage (V)
W	width of groove (m)
We	Webber number $\left(\frac{Q^2}{\rho_v D^3 h_{fg}^2 \sigma}\right)$
σ	surface tension (N/m)
θ	contact angle
ρ	density (kg/m^3)
μ	viscosity (Ns/m^2)

Subscripts

hp	heat pipe
out	outlet
in	inlet, input
e	evaporator
c	condenser
e,i	evaporator inner wall
c,i	condenser inner wall
sat	saturation

o	outer
T	total
l	liquid
v	vapor